Genes & Diseases (2019) 6, 391–397

Available online at www.sciencedirect.com

ScienceDirect

journal homepage: http://ees.elsevier.com/gendis/default.asp

SHORT COMMUNICATION

Decreased osteogenic activity and mineralization of alveolar bone cells from a patient with amelogenesis imperfecta and *FAM83H* 1261G > T mutation

Nunthawan Nowwarote [a], Thanaphum Osathanon [b], Kiattipan Kanjana [b], Thanakorn Theerapanon [a], Thantrira Porntaveetus [a,*], Vorasuk Shotelersuk [c,d]

[a] *Genomics and Precision Dentistry Research Unit, Department of Physiology, Faculty of Dentistry, Chulalongkorn University, Bangkok, 10330, Thailand*
[b] *Center of Excellence for Regenerative Dentistry, Department of Anatomy, Faculty of Dentistry, Chulalongkorn University, Bangkok, 10330, Thailand*
[c] *Center of Excellence for Medical Genomics, Department of Pediatrics, Faculty of Medicine, Chulalongkorn University, Bangkok, 10330, Thailand*
[d] *Excellence Center for Medical Genetics, King Chulalongkorn Memorial Hospital, The Thai Red Cross Society, Bangkok, 10330, Thailand*

Received 5 May 2019; received in revised form 10 July 2019; accepted 18 July 2019
Available online 29 July 2019

KEYWORDS
Autosomal dominant inheritance;
Enamel hypoplasia;
Hypocalcified enamel;
Mineralization;
Osteogenic differentiation;
Periodontium

Abstract *FAM83H* mutations lead to autosomal dominant hypocalcified amelogenesis imperfecta (ADHCAI). However, the biological role of *FAM83H* remains unclear. The present study aimed to characterize the alveolar bone cells isolated from a patient with ADHCAI having the mutation, c.1261G > T, p.E421*, in *FAM83H*. We showed that *FAM83H* mutant cells had proliferation ability and morphology similar to the controls. The F-actin staining revealed that *FAM83H* mutant cells were remained in the earlier stages of cell spreading compared to the controls at 30 min, but their spreading was advanced comparable to the controls at later stages. After osteogenic induction, a significant decrease in mRNA levels of *RUNX2* and *ALP* was observed in *FAM83H* mutant cells at day 7 compared with day 3 while their expressions were increased in the controls. The *OPN* levels in *FAM83H* mutant cells were not significantly changed at day 7 compared to day 3 while the controls showed a significant increase. After 14 days, the mineral deposition of *FAM83H* mutant cells was slightly lower than that of the controls. In conclusion, we identify that *FAM83H* bone cells have lower expression of osteogenic

* Corresponding author. Genomics and Precision Dentistry Research Unit, Faculty of Dentistry, Department of Physiology, Faculty of Dentistry, Chulalongkorn University, Bangkok 10330, Thailand. Fax: +662 218 8691.
E-mail address: thantrira.p@chula.ac.th (T. Porntaveetus).
Peer review under responsibility of Chongqing Medical University.

https://doi.org/10.1016/j.gendis.2019.07.005

marker genes and mineralization while they maintain their morphology, proliferation, and spreading. Consistent with previous studies in the ameloblasts and periodontal ligamental cells, these evidences propose that *FAM83H* influences osteogenic differentiation across different cell types in oral cavity.

Introduction

Family with sequence similarity 83 member H (*FAM83H*; OMIM * 611927) is a member of FAM83 family. Mutations in *FAM83H* are the major cause of autosomal dominant hypocalcified amelogenesis imperfecta (ADHCAI) presenting abnormal enamel mineralization.[1] Recently, *FAM83H* has been implicated in several cancers including colorectal, prostate, and hepatocellular cancers.[2–4] *FAM83H* overexpression was identified in twelve percent of head and neck squamous cell carcinoma.[5] It has also been shown to control the arrangement of the keratin cytoskeleton and formation of desmosomes.[6] These suggest the diverse roles of *FAM83H* in biological processes.

Fam83h null mice and transgenic mice overexpressing *Fam83h* did not show phenotype in enamel and dentin,[7,8] suggesting the gain-of-function or dominant negative effect of mutant FAM83H protein causing ADHCAI. Inhibition of mineralization, down-regulation of the expression of osteogenic factors, and disorganization of keratin cytoskeleton and desmosome in ameloblast cells have been proposed as the pathogenic mechanisms of ADHCAI.

In oral cavity, *FAM83H* expression was observed in the ameloblasts, odontoblasts, and alveolar bone.[9] Murine ameloblast cell line transfected with *Fam83h* mutant cDNA (c.1186C > T) exhibited a significant decrease in expression of osteogenic marker genes, namely *Runx2*, *Alp*, and *Ocn*, corresponding with the reduction of ALP activity.[10] Our previous study demonstrated that the periodontal ligament cells isolated from the ADHCAI patient with *FAM83H* mutation (p.E421*) showed impaired proliferation and down-regulation of *OCN*, *BSP*, and *COL1* levels after mineralization induction.[11] The teeth affected with ADHCAI also showed reduced mineral density. These lines of evidence show that the *FAM83H* mutant cells had impaired functions related to osteogenic differentiation and mineralization. The present study for the first time investigated the characteristics and mineralization ability of alveolar bone cells obtained from a patient with the heterozygous nonsense mutation, c.1261G > T, p.E421*, in the *FAM83H* gene.

Materials and methods

Subject enrollment

The study was approved by Institutional Review Board (IRB No. 163/61), Faculty of Medicine, Chulalongkorn University and complied with the Declaration of Helsinki. Informed consents were obtained from all participants in this study. Genetic mutation was analyzed by whole exome sequencing as described in our previous study.[11] The identified variant was validated in the proband and other family members by Sanger sequencing.

Cell isolation

Bone chips were obtained from the buccal bone plate of a patient affected with ADHCAI during surgical extraction of impacted third molars. Cell isolation was performed by explanting method. Briefly, bone chips were maintained in Dulbecco's modified eagle medium (DMEM) (Gibco, USA) supplemented with 15% fetal bovine serum, 2 mM L-glutamine, 100 U/mL penicillin, 100 μg/mL streptomycin, and 250 ng/mL amphotericin B. Cells were subcultured upon reaching confluence. These cells were considered as passage 1. The present study utilized cells at passages 3—6. The controls were alveolar bone cells at similar passage from healthy subjects.

Cell proliferation assay

MTT (3-(4,5-Dimethylthiazol-2-yl)-2,5-Diphenyltetrazolium Bromide) assay was employed to determine cell proliferation. Cells (12,500 cells) were plated in 24 well-plate and maintained in growth medium. Cells were incubated with MTT solution (1 mg/mL) for 10 min. The precipitated formazans crystals were solubilized using dimethysulfoxide solution and glycine buffer. The absorbance was monitored at 570 nm.

Immunofluorescence staining

Cells were incubated with 3% glutaraldehyde (Fluka Analytical, USA) for 10 mins. After washing with PBS, samples were treated with 0.1% Triton®-X100 (Sigma—Aldrich, USA). Samples were incubated with rhodamine-phalloidin antibody (Invitrogen, USA) in 10% horse serum and stained with DAPI.

Scanning electron microscopic (SEM)

Cells were fixed with 3% glutaraldehyde and processed through ethanol dehydration steps. Subsequently, cells were critically point dried, sputter-coated with carbon, and examined by SEM (Quanta 250, FEI, Hillsboro, OR, USA). Cell spreading was categorized into 4 stages according to previous publication.[12]

Osteogenic differentiation

Cells were seeded at the density of 50,000 cells/well in a 24-well plate. After confluency, the medium was changed to osteogenic induction medium supplemented with dexamethasone (100 n*M*), L-ascorbic acid (50 μg/mL), and β-glycerophosphate (10 m*M*). The cells were stained with alizarin red S to determine mineralization. Staining was solubilized in cetylpyridium chloride solution and the absorbance was measured at 570 nm.

Polymerase chain reaction

Total RNA was extracted by RiboEx solution (GeneAll, Korea). Reverse transcriptase kit (Promega, Madison, WI, USA) was employed to convert RNA (1 μg) to cDNA. Real-time polymerase chain reaction (RT-PCR) was performed to determine gene expression levels using FastStart® Essential DNA Green Master (Roche, USA) and MiniOpticon system (Bio-rad). Melting curve analysis was examined to ensure product specificity. Expression value was calculated using ($2^{-\Delta\Delta Ct}$) method. Primer sequences are shown in Supplementary Table 1.

Statistical analyses

The statistical analysis was performed using Prism7 (GraphPad Software, CA, USA). The significant difference between two groups was determined using Mann Whitney U test. Kruskal Wallis test followed by pairwise comparison was utilized for three or more group comparison. The statistically significant difference was considered when *p* value less than 0.05.

Results

Clinical and molecular characterisation of a patient with ADHCAI and *FAM83H* mutation

The proband, a Thai female at 21 years of age, presented with generalized yellowish porous enamel. The radiopacity of her enamel was reduced (Fig. 1A—C). Whole exome sequencing identified the heterozygous nonsense mutation (c.1261G > T, p.E421*) in exon 5 of *FAM83H* (NM_198488.3) leading to ADHCAI in the proband. This mutation was located in the frequent mutation sites between amino acid 287—694 of FAM83H (Fig. 2A). The mutation was also detected in her father and brother having the same tooth condition but not in her unaffected mother by Sanger sequencing (Fig. 2B). Clinical and radiographic features of the proband were described in our previous study.[11] Bone chips were obtained from the proband during osteoplasty according to orthodontic treatment plan.

Proliferation and spreading of *FAM83H* mutant cells

MTT assay showed that the cells obtained from the alveolar bone of the proband (called *FAM83H* mutant cells in this study) showed an increase in cell number at day 7 compared to day 1 (Fig. 1D). At day 7, their number was comparable to the controls (Fig. 1D). These show that *FAM83H* mutant cells had an ability to proliferate *in vitro*.

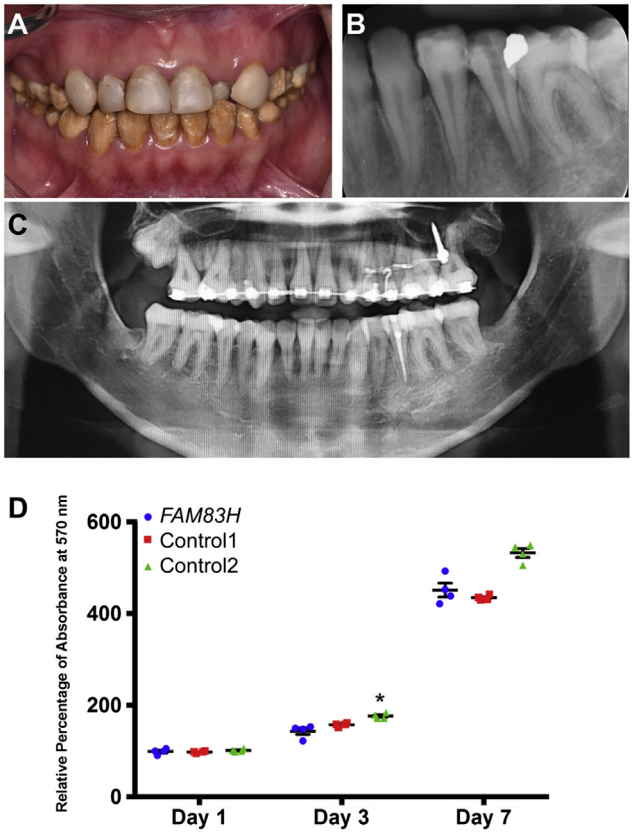

Figure 1 Clinical and radiographic features of the proband and proliferation of *FAM83H* mutant cells. Frontal view of oral photograph of the proband showed rough and yellowish enamel. The upper anterior teeth were restored with resin composite (A). Periapical radiograph of lower left posterior teeth exhibited partial loss of enamel with reduced radiopacity (B). Panoramic radiograph of the proband at age 20 years showed that the enamel of erupted teeth was thin and less radiopacity. The maxillary and mandibular bones were unremarkable (C). Cell proliferation of *FAM83H* mutant and control cells determined by MTT assay at day 1, 3, and 7 (C). Asterisk indicated the statistically significant difference between *FAM83H* mutant and control cells.

At early time points, SEM revealed that *FAM83H* mutant cells demonstrated a round shape with small filopodia and/or lamellopodia which were less extended than those of the controls (Fig. 3A—F). Later, at 6 and 24-hour culture, both *FAM83H* mutant and control cells showed flatten shape, suggesting a complete cell spreading (Fig. 3C—H). Stages of cell spreading was determined according to previous publication.[11] At 30 min, the majority of *FAM83H* mutant cells were categorized into stage 1 and 2 while the controls were in stages 2 and 3 (Fig. 3I). The *FAM83H* mutant cells progressed into stage 2, 3, and 4 at 2 h and their spreading was comparable to the controls at 6 and 24 h.

F-actin staining showed the unspecific organization of actin in the cytoplasm of both *FAM83H* mutant and control cells at 30 min (Fig. 4A—C). At 2 and 6 h, the orientation of F-actin was present around the edge of cell membrane

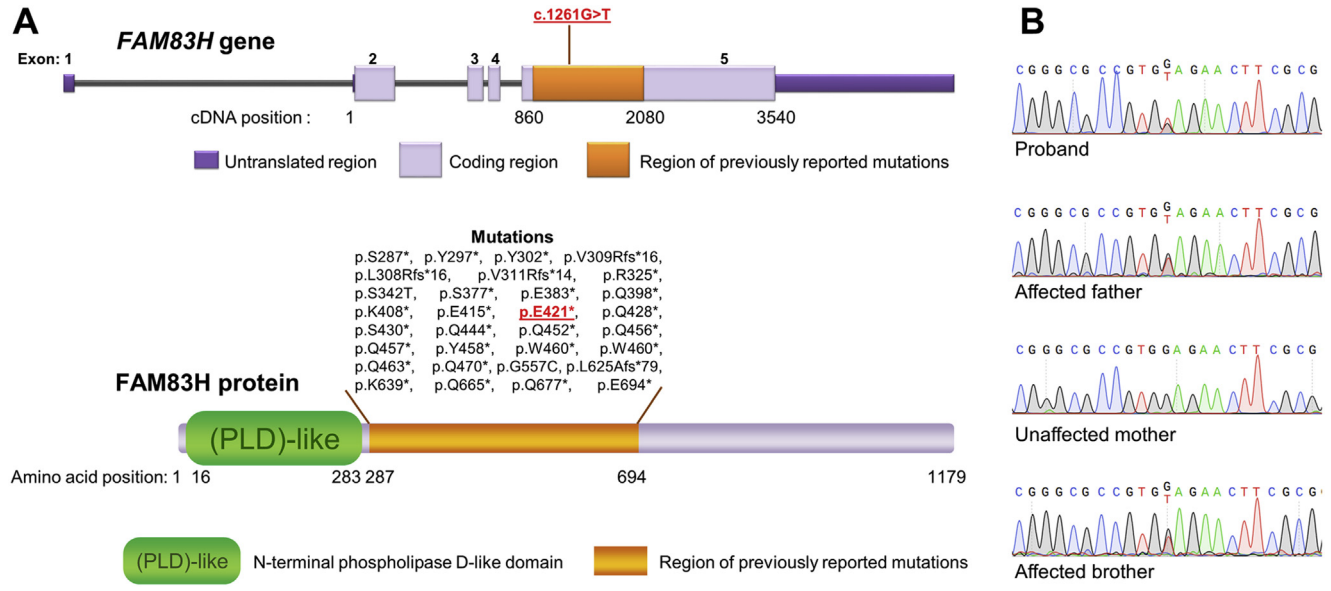

Figure 2 Mutation analysis. The schematic diagram of *FAM83H* gene (NM_198488.3) showed the location of c.1261G > T, p.E421* mutation. The structural domains of FAM83H (NP_940890.3) illustrated the previously reported mutations spanning between amino acid 287 and 694 (A). Electropherograms identified the heterozygous missense mutation, c.1261G > T, p.E421*, in the proband and her affected father and brother, but not in her mother (B).

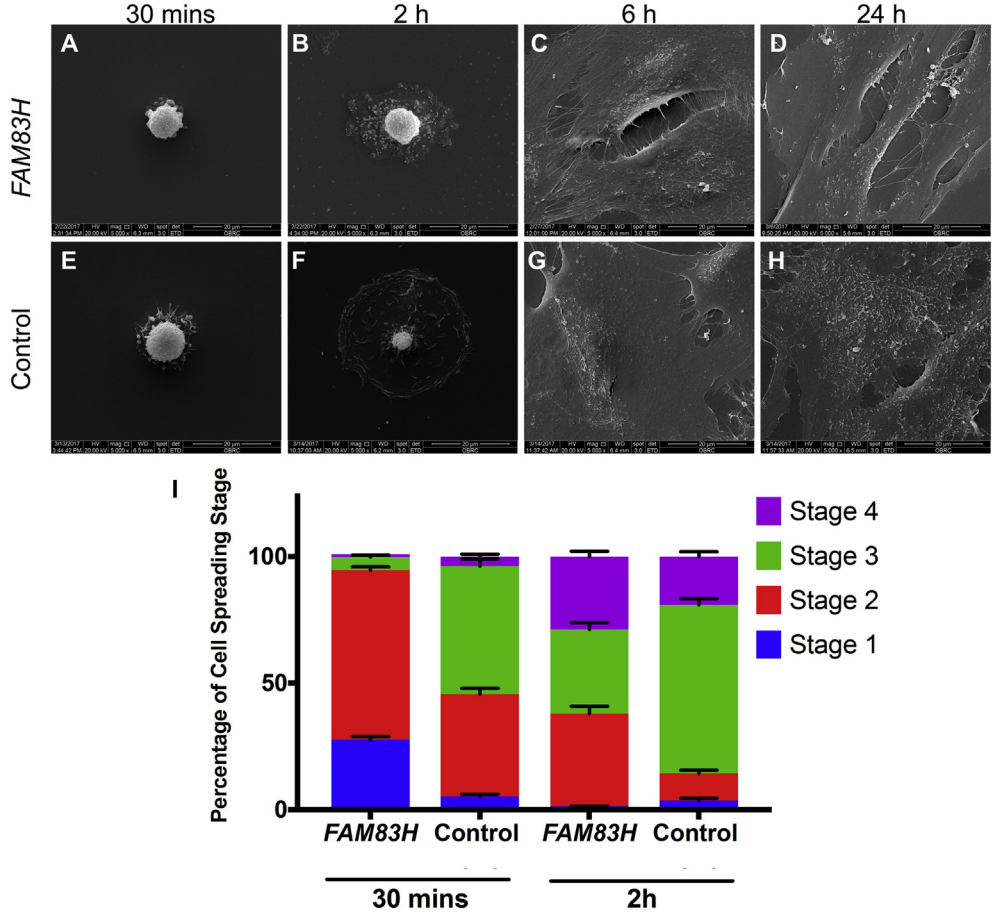

Figure 3 Cell spreading of *FAM83H* mutant cells. Morphology and cell spreading were evaluated by scanning electron microscope at 30 min (mins), 2 h (h), 6h and 24h after seeding. Representative images of *FAM83H* mutant cells (A—D) and control cells (E—H). The percentage of cell spreading stage (stage 1—4) measured at 30 mins and 2h (I).

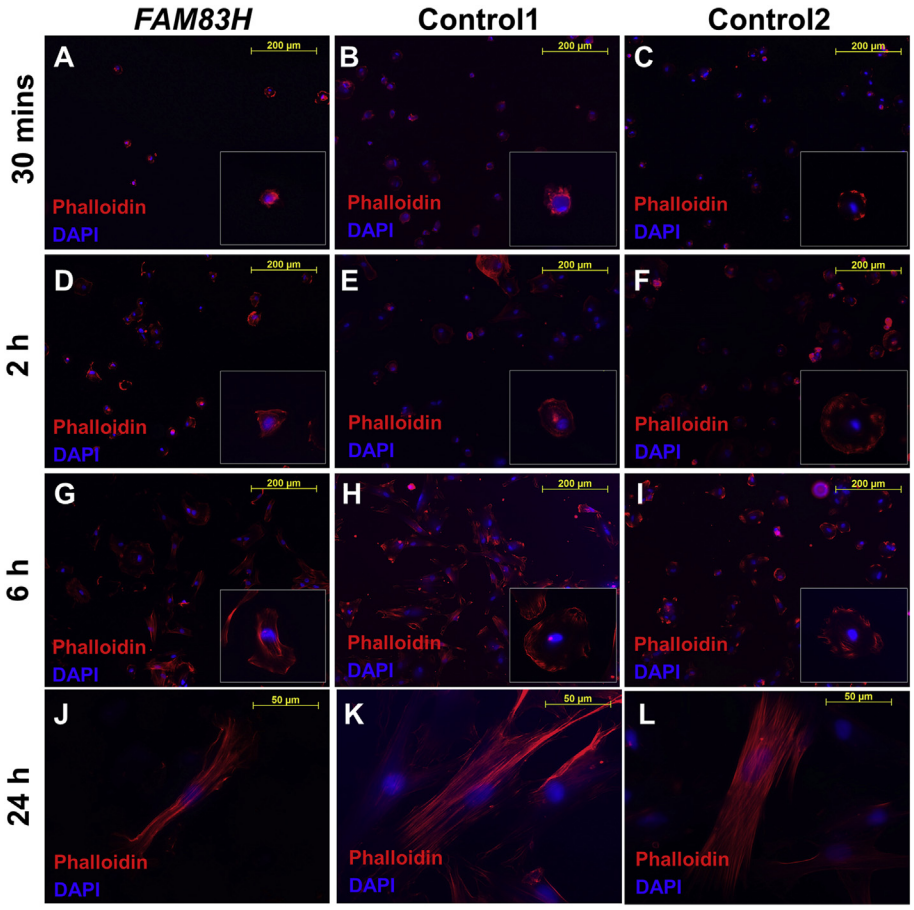

Figure 4 F-actin arrangement of *FAM83H* mutant cells. Cells seeded on tissue culture plates for 30 mins (A—C), 2h (D—F), 6h (G—I), 24h (J—L), and subsequently stained with rhodamine-phalloidin for F-actin (red) and DAPI (blue).

(Fig. 4D—I). The stress fibers were obviously detected in all groups at 24 h (Fig. 4J—L). There was no marked difference in F-actin organization between *FAM83H* mutant and control cells during this observation period.

Osteogenic differentiation of *FAM83H* mutant cells

The mRNA level of *FAM83H* was downregulated in *FAM83H* mutant cells (Supplementary Fig. 1). The expression of osteogenic markers was evaluated using RT-PCR after cells were maintained in osteogenic medium for 3 and 7 days. We observed that *FAM83H* mutant cells exhibited a significant decrease of *RUNX2* and *ALP* expression at day 7 compared with day 3 while those markers were increased in the controls (Fig. 5A,B). While the expression levels of *OPN* in *FAM83H* mutant cells were not significantly different between day 7 and day 3, the significant upregulation was found in the controls (Fig. 5C). Both *FAM83H* mutant and control cells showed significant increase of *DSPP* and *OCN* levels at day 7 compared with day 3 (Fig. 5D,E). *FAM83H* mutant cells exhibited mineral deposition but slightly lower than the controls after culturing in osteogenic induction medium for 14 days (Fig. 5F and Supplementary Fig. 2).

Discussion

FAM83H has been shown to involve in mineralization process. This study investigated the characteristics of cells obtained from the alveolar bone of a patient affected with ADHCAI and the truncating mutation (p.E421*) in *FAM83H*. We observed that *FAM83H* mutant cells had comparable morphology, proliferation, spreading, and cytoskeletal arrangement to the controls. After osteogenic induction, *FAM83H* mutant cells exhibited a slight reduction in mineral deposition and a significant decrease in the expression of osteogenic marker genes compared to the controls.

The effects of *FAM83H* on cell proliferation have been reported in several cell types. Deletion of *FAM83H* resulted in reduced proliferation and induction of G0/G1 cell cycle arrest of hepatocellular carcinoma cells.[3] Impaired cell proliferative ability was observed in human periodontal ligament cells with p.E421* mutation in *FAM83H*.[11] This study detected a significant reduction in the number of *FAM83H* mutant cells compared to control2 at day 3, however, a significant difference was not observed at day 7. These suggest that *FAM83H* mutation do not alter the proliferation ability of human alveolar bone cells and the mutation might variably influence cell proliferation depending on cell types.

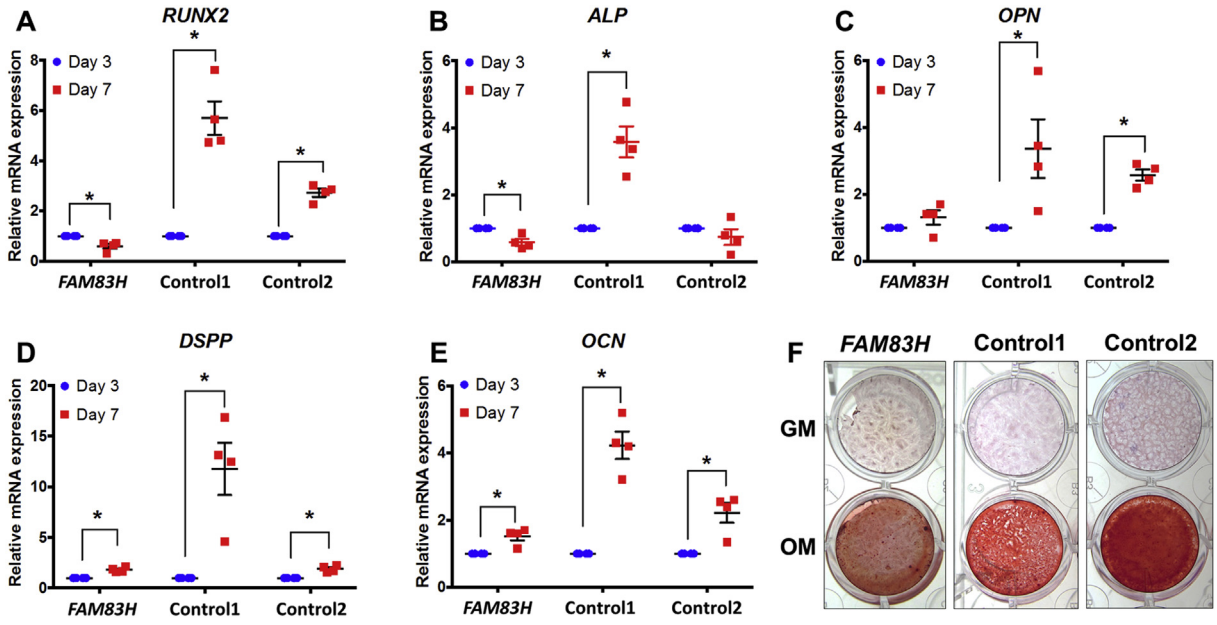

Figure 5 Osteogenic differentiation of *FAM83H* mutant cells. The mRNA expression of osteogenic marker genes examined by RT-PCR at day 3 and 7 (A—E). Mineral deposition shown by alizarin red s staining at day 14 after osteogenic induction (F).

Previous report demonstrated that mouse ameloblast cells with *Fam83h* mutation (c.1186C > T, p.Q396*) exhibited lower expression of *Runx2*, *Alp*, and *Ocn* and ALP activity than the controls after osteogenic induction.[10] Those expression levels were rescued by Wnt signaling inhibitor.[10] In humans, the periodontal ligamental cells with *FAM83H* mutation exhibited a decrease in *BSP*, *COL1*, *OCN* mRNA expression.[11] Consistently, this study detected that human alveolar bone cells with *FAM83H* mutation had a significant decrease in *RUNX2* and *ALP* and unchanged *OPN* expression at day 7 compared with day 3 while the controls showed a significant upregulation of those markers. The expression of *DSPP* and *OCN* in *FAM83H* mutant and control cells was upregulated at day 7 comparing with day 3 in which *FAM83H* mutant cells showed lower fold changes. Taken together, these suggest that multiple types of cells with *FAM83H* mutation had compromised ability in osteogenic differentiation.

We found that the mineral deposition of *FAM83H* mutant cells was slightly lower than the controls. An *in vitro* mineralization has been shown to be associated with osteogenic differentiation potency but the regulatory mechanisms of each can be independent. For example, inorganic phosphate regulation has been shown to independently promote mineralization and differentiation.[13] The control of local crystal nucleation and growth is crucial for mineralization process but may not directly associate with osteogenic differentiation.[14] Hence, the roles of *FAM83H* in mineralization process across different types of cells should be further elucidated.

In conclusion, we show that *FAM83H* alveolar bone cells have reduced expression of osteogenic markers and slight decrease in mineral deposition, suggesting their compromised ability in osteogenic differentiation. The morphology, proliferation, spreading, and cytoskeleton of *FAM83H* bone cells are comparable to those of the controls. Consistent with previous studies in the ameloblasts and periodontal ligamental cells, our findings propose an influence of *FAM83H* on the osteogenic differentiation across cell types in oral cavity.

Conflict of interest

None.

Acknowledgements

The study was supported by the Medical Genomics Cluster of Chulalongkorn University, Chulalongkorn Academic Advancement Into Its 2nd Century Project, Newton Fund, and Thailand Research Fund (RSA6280001, DPG6180001, RSA6180019). Nunthawan Nowwarote is supported by the Ratchadapisek Sompote Fund for Postdoctoral Fellowship, Chulalongkorn University. We thank Trakarn Sookthonglarng and Yuttupong Kunchanapruek for blood collection, Lawan Boonprakong and Anucharte Sirjunbarl for microscope services.

Appendix A. Supplementary data

Supplementary data to this article can be found online at https://doi.org/10.1016/j.gendis.2019.07.005.

References

1. Kim J-W, Lee S-K, Lee ZH, et al. FAM83H mutations in families with autosomal-dominant hypocalcified amelogenesis imperfecta. *Am J Med Genet*. 2008;82(2):489—494.
2. Snijders AM, Lee SY, Hang B, Hao W, Bissell MJ, Mao JH. FAM83 family oncogenes are broadly involved in human cancers: an

integrative multi-omics approach. *Mol Oncol*. 2017;11(2):167—179.
3. Kim KM, Park SH, Bae JS, et al. FAM83H is involved in the progression of hepatocellular carcinoma and is regulated by MYC. *Sci Rep*. 2017;7(1):3274.
4. Kuga T, Kume H, Kawasaki N, et al. A novel mechanism of keratin cytoskeleton organization through casein kinase Iα and FAM83H in colorectal cancer. *J Cell Sci*. 2013;126(20):4721—4731.
5. Lepikhova T, Karhemo PR, Louhimo R, et al. Drug sensitivity screening and genomic characterization of 45 HPV-negative head and neck carcinoma cell lines for novel biomarkers of drug efficacy. *Mol Cancer Ther*. 2018;17(9):2060—2071.
6. Kuga T, Sasaki M, Mikami T, et al. FAM83H and casein kinase I regulate the organization of the keratin cytoskeleton and formation of desmosomes. *Sci Rep*. 2016;6:26557.
7. Wang SK, Hu Y, Yang J, et al. Fam83h null mice support a neomorphic mechanism for human ADHCAI. *Mol Genet Genom Med*. 2016;4(1):46—67.
8. Kweon YS, Lee KE, Ko J, Hu JC, Simmer JP, Kim JW. Effects of Fam83h overexpression on enamel and dentine formation. *Arch Oral Biol*. 2013;58(9):1148—1154.
9. Lee MJ, Lee SK, Lee KE, Kang HY, Jung HS, Kim JW. Expression patterns of the Fam83h gene during murine tooth development. *Arch Oral Biol*. 2009;54(9):846—850.
10. Yang M, Huang W, Yang F, Zhang T, Wang C, Song Y. Fam83h mutation inhibits the mineralization in ameloblasts by activating Wnt/beta-catenin signaling pathway. *Biochem Biophys Res Commun*. 2018;501(1):206—211.
11. Nowwarote N, Theerapanon T, Osathanon T, Pavasant P, Porntaveetus T, Shotelersuk V. Amelogenesis imperfecta: a novel FAM83H mutation and characteristics of periodontal ligament cells. *Oral Dis*. 2018;24(8):1522—1531.
12. Osathanon T, Bespinyowong K, Arksornnukit M, Takahashi H, Pavasant P. Human osteoblast-like cell spreading and proliferation on Ti-6Al-7Nb surfaces of varying roughness. *J Oral Sci*. 2011;53(1):23—30.
13. Osathanon T, Nowwarote N, Manokawinchoke J, Pavasant P. bFGF and JAGGED1 regulate alkaline phosphatase expression and mineralization in dental tissue-derived mesenchymal stem cells. *J Cell Biochem*. 2013;114(11):2551—2561.
14. Addison WN, Azari F, Sorensen ES, Kaartinen MT, McKee MD. Pyrophosphate inhibits mineralization of osteoblast cultures by binding to mineral, up-regulating osteopontin, and inhibiting alkaline phosphatase activity. *J Biol Chem*. 2007;282(21):15872—15883.